"Speciation of platinum nanoparticles in different cell culture media by HPLC-ICP-TQ-MS and complementary techniques: a contribution to toxicological assays"

Sergio Fernández-Trujillo, Nuria Rodríguez-Fariñas, María Jiménez-Moreno,

Rosa del Carmen Rodríguez Martín-Doimeadios*

Department of Analytical Chemistry and Food Technology, Faculty of Environmental Sciences and Biochemistry, University of Castilla-La Mancha, Avenida Carlos III s/n, 45071 Toledo, Spain.

*Corresponding author:

Prof. Dr. Rosa del Carmen Rodríguez Martín-Doimeadios

Rosacarmen.rodriguez@uclm.es

Abstract

Toxicological studies of nanoparticles (NPs) are highly demanded nowadays but they are very challenging. In the *in vitro* assays, the understanding of the role of cell culture media is crucial to derive a proper interpretation of the toxicological results and to do so, new analytical tools are necessary. In this context, an analytical strategy based on reversed-phase liquid chromatography hyphenated to inductively coupled plasma-triple quadrupole mass spectrometry (HPLC-ICP-TQ-MS) has been developed for the first time for the detection and characterization of both 5 and 30 nm PtNPs, as well as ionic platinum species, in commonly used cell culture media. For this purpose, Dulbecco's Modified Eagle Medium, DMEM-high glucose, DMEM-F12, DMEM 31053-028, and Roswell Park Memorial Institute, RPMI-1640 (supplemented with 10% fetal bovine serum (FBS) and antibiotics) at several incubation times (24, 48, and 96 h at 37°C) were tested. After a careful optimization and analytical performance, the developed method allows to simultaneously study the oxidation process, leading to the release of ionic species, and the increase in the hydrodynamic volume of PtNPs, probably related to the formation of new biological entities (protein corona). The magnitude of both processes was found to be dependent on the tested cell culture media and incubation times. Dynamic light scattering (DLS) and high-resolution scanning electron microscopy (HR-SEM) were used as complementary techniques to study the important process of both soft and hard protein corona formation. The feasibility of the HPLC-ICP-TQ-MS to get relevant information for toxicological studies has been demonstrated and in light of our results, the influence of the cell culture media on the behavior of PtNPs should not be underestimated.

Keywords: reversed-phase liquid chromatography; inductively coupled plasma mass spectrometry; platinum nanoparticles; cell culture media; toxicological assays.

1. Introduction

Platinum nanoparticles (PtNPs) stand out because of their unique structural, optical, and catalytic properties which make them be used in numerous fields with high social impact, including nanomedicine, where they are considered as promising antimicrobial and anticancer agents, or for targeted drug delivery [1,2]. Due to their numerous potential applications, the exposure to these nano-sized particles is expected to increase substantially in the next years, but their impact on human health is little known today and should not be overlooked [3].

There is an increasing demand for toxicological studies, and the *in vitro* approach is the first step [4,5]. In these studies, NPs are in contact with cells grown in culture media, often supplemented with nutrients and antibiotics. In this highly complex biological media, NPs do not behave as inert entities, but they undergo different transformations, such as aggregation/agglomeration, adsorption of biomolecules, ion release, and others [6-13]. A number of biological responses at cellular level depend on these processes, so their full understanding is essential to achieve a correct interpretation of the toxicological results. To tackle this issue, characterization of NPs, especially in terms of size, is a reasonable strategy to track the transformations they undergo in culture media. Characterization of NPs is inherently complicated because of the dynamics of these processes, but above all, because of the different composition of cell culture media. The variations in their aminoacid, glucose, or salt composition are significant and definitely influence these transformations and interactions [6,12].

Different techniques have been traditionally used for characterization of NPs, mainly based on microscopy (transmission electron microscopy (TEM), scanning electron microscopy (SEM), and atomic force microscopy (AFM)), spectroscopy (dynamic light scattering (DLS), Raman, and ultraviolet-visible spectroscopy (UV-vis)) and, more recently, strategies based on inductively coupled plasma-mass spectrometry (ICP-MS) for metallic NPs in various acquisition modes [14-18]. Potentials and drawbacks of each technique for this particular use have been extensively reviewed and discussed, and the main conclusion is that a single technique cannot provide all the requested information in these complex samples; rather a battery of techniques that provide complementary data are necessary to get a full picture [19].

In this context, it is of special interest the analytical approach based on the use of separation techniques coupled to elemental specific detectors such as ICP-MS, i.e., capillary electrophoresis (CE), high performance liquid chromatography (HPLC), and field flow fractionation (FFF) [8,9,14,20-22]. Among these hyphenated techniques, HPLC-ICP-MS is attracting increasing attention since it was firstly proposed by Helfrich et al. (2006) [23]. This technique provides information about changes in NP size due to interactions with the culture media as well as about NP dissolution, i.e., ion release, in a simultaneous manner and with minimum sample treatment. All this helps understand if the toxicological effects are due to the NPs, ions, or both, and nearly no other technique can provide this information. Moreover, low limits of detection (LODs) are reached, and the instrumentation is quite simple, cost-effective, and easy to transfer to toxicological laboratories. In the last years, this approach has been used mainly for gold nanoparticles (AuNPs) [8,11,21-27], and silver nanoparticles (AgNPs) [21,25,28,29], in some environmental and biological samples, with minor attention to PtNPs [21]. As far as we know, despite the benefits on offer, this analytical approach has never been exploited for PtNP characterization in complex biological samples such as cell culture media used in *in vitro* toxicological studies.

Hence, the aim of this work is the development of an analytical methodology based on HPLC-ICP-MS for the study of PtNPs and platinum (Pt) ionic species in different cell culture media, namely Dulbecco's Modified Eagle Medium (DMEM-high glucose, DMEM-F12 and, DMEM 31053-028), and Roswell Park Memorial Institute (RPMI-1640), supplemented with 10% fetal bovine serum (FBS) and antibiotics as they are commonly used in nanotoxicological assays. The PtNP transformations will be also monitored by complementary spectroscopic (dynamic light scattering (DLS)), and microscopic (high-resolution scanning electron microscopy (HR-SEM)) techniques.

2. Material and methods

2.1. Reagents

All chemicals and reagents were of analytical grade and solutions were prepared in ultrapure water (18.2 MΩ cm) obtained from a Milli-Q® A10TM water purification

system (Millipore Corporation, USA). Commercial solutions of spherical PtNPs (5, and 30 nm) stabilized in 2 mM citrate were purchased from nanoComposix (USA). They were characterized for concentration and size. Quantitative analysis was by ICP-TQ-MS after microwave digestion (53.4±0.8 and 60±2 μg mL^{-1} (*n*=3) for 5 and 30 nm PtNPs, respectively) as previously described [30]. The estimated size by HR-SEM was 31±3 nm (*n*=400) for the 30 nm PtNP (**Figure S1**). No data are given for 5 nm PtNPs because it is below the size limit (ca. 10 nm) of the equipment used. The TEM report from the supplier verified monodispersed PtNPs with nominal diameters of 4±0.7 nm and 30±3 nm.

Rhodium (995±2 μg mL^{-1} of Rh in 2.5% HNO_3) and Pt (1000±3 μg mL^{-1} of Pt in 5% HCl) solutions were acquired from Inorganic Ventures (USA). HCl (37%), methanol and $NaH_2PO_4 \cdot H_2O$ were purchased from Scharlab (Spain). HNO_3 (69%), $Na_2HPO_4 \cdot 12H_2O$ and TWEEN® 20 were obtained from Merck (Germany). Hexadecyltrimethylammonium bromide (CTAB) and Sodium dodecyl sulphate (SDS) were acquired from Acros Organics (Spain). Dulbecco's Modified Eagle Medium (DMEM)-high glucose, DMEM-Ham's F-12 (DMEM F12), fetal bovine serum (FBS), penicillin, and streptomycin were obtained from Lonza (Spain). DMEM 31053-028, and Roswell Park Memorial Institute medium (RPMI-1640) were purchased by Thermo Fisher Scientific (Germany). A description of the most relevant cell culture media compounds is given in **Table S1.**

2.2. Apparatus and instrumental features

An ICP-TQ-MS system (iCAP TQ, Thermo Fisher Scientific, Germany) equipped with a Micro Mist nebulizer and a cyclonic spray chamber was used. The single quadrupole kinetic energy discrimination mode (SQ-KED) was selected with He as collision gas. The instrument was tuned daily for the highest sensitivity. Rhodium (15 μg L^{-1}) was simultaneously aspirated during the ICP-TQ-MS data acquisition, and it was used to correct signal drifts. The raw data of the transient isotope signal for the different PtNPs and Rh (internal standard) were processed using the Qtegra™ Intelligent Scientific Data Solution™ (ISDS) software.

An HPLC system was coupled to ICP-TQ-MS detector. A high-pressure quaternary gradient pump (Jasco PU-2089, Japan) was used. Separation was performed in a reversed-phase C18 column (Nucleosil 7 μm particle size, 1000 Å pore size, 250×4.6 ID

mm, Machery-Nagel, Germany) at a flow rate of 0.5 mL min^{-1}. A sample injection valve (Rheodyne 7725i, Rohnert Park, CA, USA) fitted with a loop of 20 µL was used. The mobile phase consisted of phosphate buffered saline (PBS, 2 mM, pH = 7.3) with the addition of SDS (10 mM). It was filtered through 0.45 µm hydrophilic nylon membrane filters (Millipore, Spain) and degassed.

The optimum HPLC-ICP-TQ-MS program is summarized in **Table 1**.

A Zeiss GeminiSEM 500 instrument (Germany) with a maximum acceleration voltage of 30 kV was used to obtain high-resolution SEM (HR-SEM) micrographs. The nano-sized solutions were deposited on silicon wafers and allowed to dry for 24 h prior to measurement.

A Malvern Zetasizer Nano ZS (Malvern Panalytical, UK) was used to obtain information on the PtNP hydrodynamic diameter. The DLS measurements were carried out using a dust-free disposable cuvette (DTS0012, Malvern Panalytical, UK). The volume was 1 mL, the backscatter angle was 173°, and the temperature 25°C (after equilibration for 2 min). Three consecutive measurements were performed using a minimum of 11 runs. The DLS characteristics of the measured sample, given as Z-average size, were determined by averaging the replicate values (*n*=3).

An advanced ZX3 Vortex (Velp Scientifica, Italy), and an ultracentrifuge Digicen 21R (Orto Alresa, Spain) were employed.

A CO_2 incubator (HEPA Class 100, Thermo Fisher Scientific, USA) was employed for incubation experiments.

2.3. Preparation of PtNPs without and with cell culture media

The PtNPs were prepared without and with cell culture media as previously reported with some modifications [9]. Briefly, these nano-sized particles were homogenized with vortex agitation at 1,200 rpm for 1 min before use. In the experiments without cell culture media, the PtNPs were diluted in mobile phase. For the experiments with cell culture media, the PtNPs were diluted in DMEM-high glucose, DMEM F-12, DMEM 31053-028, or RPMI-1640 (supplemented with 10% of FBS, 100 U

mL^{-1} penicillin and 100 µg mL^{-1} streptomycin), and directly injected (experiments at time = 0 h) or incubated at different times (24, 48, and 96 h) at 37°C.

In all cases, the standards and samples were homogenized by vortex agitation for 10 s and filtered through 0.2 mm nylon filters before injection into the HPLC-ICP-TQ-MS system.

2.4. Protein corona preparation

The 30 nm PtNPs were dispersed (dilution 1:1) in DMEM-high glucose or RPMI-1640 following the procedure described by Strojan et al. (2017) with some modifications to study the protein corona formation around the NPs [10]. These suspensions were vortexed and incubated for 1 h at 37°C. Then, they were centrifuged at 15,000 *g* for 20 min at 4°C and the supernatants were removed. The pellets were dispersed in 1 mL of 2 mM PBS (pH = 7.3) without SDS and analysed by DLS and HR-SEM. DMEM-high glucose and RPMI-1640 suspensions without addition of the nano-sized particles were used as control.

3. Results and Discussion

3.1. Optimization of the HPLC-ICP-TQ-MS method

According to the literature related to HPLC for metallic NPs, a C18 column with 1000 Å pore size was selected in the present study for PtNPs and the ions released from them [8,21-26,28]. The separation is based on a size-exclusion mechanism according to their hydrodynamic volume, where the larger entities elute first. It is necessary to carefully optimize the composition of the mobile phase and the instrumental conditions. For the optimization, we have worked with 5 nm (50 µg L^{-1}), 30 nm (200 µg L^{-1}) PtNPs, and ionic Pt (15 µg L^{-1}) all in mobile phase.

Firstly, PBS (1 mM at pH = 7.3) was tested as mobile phase, but a strong interaction with the stationary phase of the column was observed and the addition of a surfactant was required. Thus, cationic (CTAB), anionic (SDS), and non-ionic (TWEEN® 20) surfactants were studied at different concentrations (1, 5, and 10 mM for CTAB; 5, and 10 mM for SDS, and 0.06 mM for TWEEN® 20) in presence of PBS. The separation

was not possible in the case of CTAB and TWEEN® 20 (data not shown), while the presence of SDS allowed the elution of the analytes from the column without any apparently irreversible adsorption on the packaging material **(Figure S2)**. This chromatographic behaviour is consistent with previous studies of metallic NPs in complex biological and environmental matrices [8,11,21-24,26-28]. Moreover, an increase in the relative signal intensity was observed as the SDS concentration increases **(Figure S2)**. Concentrations higher than 10 mM SDS were not considered since an excessive amount could induce depositions on the cones with deleterious effects on the ICP-TQ-MS sensitivity.

Then, different PBS concentrations (1-3 mM) were studied at pH 7.3 in the presence of 10 mM SDS. In the case of 3 mM PBS, the separation was not possible for these PtNPs mixture. Slight differences were observed in terms of signal intensity between 1 and 2 mM. Then, the recovery of the C18 column was estimated (n=6) for both PBS concentrations by quantification of total Pt by ICP-TQ-MS [8]. As for the 5 nm PtNPs, they were both satisfactory (100±2% and 100±5% for 2 mM and 1 mM, respectively). In the case of 30 nm PtNPs, significantly better results were obtained for 2 mM (66±2%) than for 1 mM PBS (43±1%). Additionally, the effect of the presence of methanol (2%) in the mobile phase was tested to improve the ionization process in the system as described elsewhere [11] but no improvement was found.

Finally, the flow rate as a key parameter affecting the separation process was studied (0.3-0.5 mL min^{-1}). **Figure S3** shows the overlapped chromatograms obtained at different flow rates for 5 nm PtNPs and ionic Pt **(Figure S3A)**, and 30 nm PtNPs and ionic Pt **(Figure S3B)**. The best separation along with a decrease in retention times is found for 0.5 mL min^{-1}.

Under the optimum conditions (Table 1), the separation of 5, 30 nm PtNPs, and its corresponding ion was achieved in less than 8 min **(Figure 1).** The retention times were 4.4, 5.3, and 6.4 min for 30, 5 nm PtNPs, and ionic Pt species, respectively. It indicates that HPLC-ICP-TQ-MS could distinguish these particles at nanoscale level from its ionic species simultaneously.

3.2. Analytical performance of the HPLC-ICP-TQ-MS methodology

The performance of the proposed analytical strategy was evaluated in terms of sensitivity, linearity, and reproducibility both without and with cell culture media for 5, 30 nm PtNP, and ionic Pt individually. The limits of detection (LOD) and quantification (LOQ) were established as the sample concentration in mobile phase that caused a peak with a height 3-fold and 10-fold the baseline noise level, respectively.

Without the cell culture media, the LODs were 1.3, 2.4, and 0.3 μg L^{-1}, whereas LOQs were 4.5, 7.9, and 0.9 μg L^{-1}, for 5, 30 nm PtNPs, and ionic Pt, respectively **(Table 2).** As can be seen in Table 2, in terms of linearity, a good correlation coefficient (R^2 > 0.999) of 5 and 30 nm PtNPs (50-500 μg L^{-1}) and ionic Pt (10-25 μg L^{-1}) was obtained. The reproducibility in terms of peak area was evaluated for 5 (50 μg L^{-1}), 30 nm (200 μg L^{-1}) PtNPs and ionic Pt (15 μg L^{-1}) as the relative standard deviation (% RSD) of replicate (*n*=6) measurements of intra-day and inter-day assays with measurement in the same day and consecutive days, respectively. The intra-day % RSD values were 0.9, 2.5, and 3.2, whereas the inter-day % RSD were 1.0, 3.0, and 3.3, for 5, 30 nm PtNPs, and ionic Pt, respectively, demonstrating the adequate repeatability and reproducibility of the developed methodology.

The performance of the HPLC-ICP-TQ-MS approach was also checked in presence of DMEM-high glucose (**Table 2**). The LODs and LOQs were higher than without the media but still in the low μg L^{-1} range (**Table 2**). The intra-day % RSD values (*n*=6) for 5 nm (50 μg L^{-1}), 30 nm PtNPs (200 μg L^{-1}), and ionic Pt (15 μg L^{-1}) were now 2.0, 5.4, and 2.6, whereas the inter-day % RSD (*n*=6) were 2.0, 5.9, and 3.2. The relative signal intensities were directly proportional to the studied concentrations with good determination coefficients (R^2 > 0.999), which demonstrated the feasibility of the proposed method. However, the slopes were significantly lower in presence of DMEM-high glucose (t-test, 95% confidence level). Experiments without HPLC were carried out to investigate if the slope decrease is related to acquisition problems in the detection by ICP-TQ-MS. Thus, calibration curves (in the range of 25-500 μg L^{-1}) of 5 and 30 nm PtNPs were prepared with and without cell culture media and measured by ICP-TQ-MS (**Table S2**). No statistically significant differences were found (t-test, 95% confidence level). Therefore, no matrix effect was found for the signal acquisition by ICP-TQ-MS, and the

observed differences should be related to the chromatographic separation and NP transformations. This result was also confirmed for RPMI-1640 (**Table S2**). The behind processes responsible for these differences will be studied in the following sections.

3.3. Study of PtNP transformations in cell culture media

The effect of different cell culture media (described in section 2.3) on the behaviour of PtNP (5, and 30 nm) was studied using the developed HPLC-ICP-TQ-MS methodology. All the tested media were supplemented with 10% FBS and antibiotics.

3.3.1. The effect of DMEM-high glucose

Initial tests were carried out using 5 (50 µg L^{-1}), 30 (200 µg L^{-1}) nm PtNPs, and ionic Pt (15 µg L^{-1}) individually in presence and absence of DMEM-high glucose directly injected into the HPLC-ICP-TQ-MS system (0 h). **Figure 2** shows the chromatograms obtained. Significant changes were found for 5 and 30 nm PtNPs **(Figures 2A and 2B)**, while the chromatographic profile, retention time and signal intensity remained nearly constant for the ionic Pt **(Figure 2C)**.

For the 5 nm PtNPs, a clear shift to lower retention times (from 5.3 to 4.2 min) is observed in presence of the biological media **(Figure 2A)**. This change can be related to an increase in size due to the adsorption onto the NP surface of matrix components, mainly proteins. This process has already been described for AuNPs in the same cell culture media by HPLC-ICP-MS [8], and for AgNPs and AuNPs by AF4-ICP-MS [7,9]. Regarding 30 nm PtNPs, only a slight shift to lower retention times (from 4.4 to 4.1 min) was observed **(Figure 2B)**. This finding suggests that 30 nm PtNPs might have increased their size so much that they could be out of the separation range of the column. Other authors have reported that metallic NPs with hydrodynamic diameter larger than 40 nm did not behave according to size exclusion theory in 1000 Å C18 column, such as the one used in the present study [21,25]. These NPs may also be retained in the column due to possible interactions with stationary phase material, especially within the small pores and thereby leading to a poor recovery.

Another important finding was the change in the chromatographic profile of the NPs **(Figures 2A and 2B)**, with an additional peak at 6.4 min in presence of DMEM. This peak could correspond to ionic Pt species released from the PtNPs since its retention time matched the ionic Pt standard **(Figure 2C)**. This phenomenon is probably related to an oxidation process of these nano-sized particles induced by the composition of the biological media (e.g., proteins, amino acids, glucose, and salts). The oxidation process has been reported in this cell culture media and cells for AuNPs (10 nm) by HPLC-ICP-MS [8] and AF4-ICP-MS [9], and for AgNPs (15 nm) by AF4-ICP-MS [7]. It is necessary to discriminate if the ionic species are coming from the NP commercial solution. The HPLC-ICP-TQ-MS system directly provides evidence of no ionic Pt in the commercial solution **(Figures 2A and 2B,** chromatograms without cell culture media), while complementary techniques, such as centrifugal ultrafiltration, are required if AF4 systems are used [9]. Therefore, the fact that this process occurs in presence only of the cell culture media should be considered to derive a correct interpretation of the observed results from toxicological studies with cells.

To have more details about these processes, experiments were conducted with different concentrations of 5, and 30 nm PtNPs (50-500 µg L^{-1}) and ionic Pt (10-25 µg L^{-1}) **(Figure S4).** As expected, the signal increases as the concentrations do. The behavior previously observed **(Figure 2)** for one concentration is confirmed for the others **(Figure S4)**. Moreover, the ionic Pt calibration curve has been used to estimate the concentration of this species in the 5, and 30 nm PtNPs chromatograms. Concentrations higher than the LODs were obtained for 200 µg L^{-1} (3.5±0.1 and 2.0±0.1 µg L^{-1}, for 5 and 30 nm respectively) and 500 µg L^{-1} (15.7±0.2 and 6.4±0.3 µg L^{-1}, for 5 and 30 nm respectively). In both cases the generation of the ionic species is more important for 5 nm than for 30 nm PtNPs. A more efficient oxidation of small NPs was also reported, probably related to their higher surface to volume ratio and reactivity [8].

Apart from the changes in the chromatographic profile, it is also remarkable the significant decrease of the signal intensity, of approximately 10 times for 5 nm **(Figure 2A)** and far more evident (approximately 40 times) for 30 nm PtNPs **(Figure 2B)**, in presence of the cell culture media. Matrix effect in the ICP-TQ-MS acquisition was discarded, as explained in section 3.2. This decrease was reported for other NPs using

either HPLC or AF4 hyphenated systems, but was not thoroughly discussed [7,9]. It could be related to the formation of entities with size out of the separation range of the LC column due to the protein adsorption and/or the formation of aggregates/agglomerates. As they are larger entities, they could also be retained in the column and therefore, it leads to a decrease in the signal intensity. This important process will be studied in the following sections in other cell culture media, apart from DMEM-high glucose, and with complementary techniques.

3.3.2. Effect of different cell culture media

Apart from DMEM-high glucose, other cell culture media commonly used have also been tested: DMEM F-12 (with HEPES, and L-Glutamine), DMEM 31053-028 (with high glucose and without HEPES and L-Glutamine), and RPMI-1640 (without HEPES and L-glutamine). All these biological media were supplemented with 10% FBS and antibiotics as previously described. In general, similar chromatographic profile and changes in retention times were observed in all the studied media **(Figure 3)**. The decrease in the signal of the NP peaks was evident in all cases, but even more important in DMEM-high glucose than in RPMI-1640 with intermediate values for the other DMEM types.

The ionic Pt was quantified for the 30 nm PtNPs in all the cell culture media. It was significantly higher for RPMI-1640 (5.7±0.2 μg L^{-1}) than for DMEM media (2.0±0.1, 2.1±0.1 and 3.7±0.2 μg L^{-1} for DMEM-high glucose, DMEM- 31053-028 and DMEM F-12, respectively). As for the 5 nm PtNPs, it was under the LOD, probably because of the low NP concentration (50 μg L^{-1}) used in this experiment. Unfortunately, as far as we know there is no literature about this process in different cell culture media to compare with.

All these findings demonstrated that the metallic NP behavior was affected by the nature of the cell culture media. The changes induced in NPs may alter the biological processes in which they are involved and, consequently, the response in cellular models. Therefore, this factor should not be overlooked to get a correct interpretation of the toxicological results.

3.3.3. Effect of the incubation time

One of the major features in toxicological assays is exposure time. Thus, the influence of incubation time (24, 48, and 96 h) at physiological temperature (37°C) was specifically tested for 5, and 30 nm PtNPs individually. DMEM-high glucose and RPMI-1640 were selected for this study.

Figure 4 shows the chromatograms of 5 nm PtNPs (50 µg L^{-1}) dispersed in DMEM-high glucose **(Figure 4A)** and RPMI-1640 **(Figure 4B)** at different incubation times (0-96 h). Data for 30 nm PtNPs (200 µg L^{-1}) are shown in **Figure S5**. The same profile and retention times were observed at least up to 96 h exposure time. However, the changes in signal intensity were more significant. The signal increased at 24 h and subsequently decreased at intermediate incubation times, far more evident for 5 nm and RPMI media **(Figure 4B)**. Therefore, dynamic changes are happening over time, and they should be properly considered. This process was also observed by Casals et al. (2010) for AuNPs in DMEM-high glucose [34]. They described transient complexes with different sizes and surface states due to competitive binding with proteins of media to form protein corona.

The peak corresponding to ionic Pt is present in all the NPs and conditions tested **(Figures 4 and S5).** There are minor changes in the signal, but it is observed a slight shift to shorter retention times at longer incubation times. This could be related to an increase in size because of adsorption of components of the cell culture media, mainly proteins. The importance of incubation time for this process has also been previously described by López-Sanz et al. (2017) for AuNPs being even more evident [8].

Therefore, the presence of NPs in contact with cell culture media at different incubation times induces changes that should be known and controlled.

3.3.4. Study by complementary techniques of protein corona in cell culture media

To have a closer insight into the processes underlying the size changes previously observed by HPLC-ICP-TQ-MS in the presence of the cell culture media, experiments to specifically study the protein corona formation have been conducted with complementary techniques such as DLS and HR-SEM [31,32].

The protein corona is a dynamic multi-layered structure formed by proteins adsorbed onto the surface of NP upon contact with biological media, such as cell culture. This structure is described to have two parts, designated as “hard” and “soft” corona [33]. The hard corona is the inner layer; it is formed by high affinity proteins and the NP-protein bonding is strong. The soft corona is the outer layer in equilibrium with the free proteins in the media. It is constituted by proteins with a lower affinity for the NP surface which form weak bonds. Hence, hard corona is a more stable complex over time than soft corona. In practice, the hard corona can be defined as those proteins which are not removed from the surface of NP during preparation procedures with a purification step (such as centrifugation).

The soft corona has been studied by DLS for 30 nm PtNPs in presence of DMEM-high glucose and RPMI-1640 (**Table S3**). No data are given for 5 nm PtNPs because it is below the size LOD for this technique (which is about 10 nm). DLS analyses confirmed that there is no evidence of aggregation/agglomeration in these media because the polydispersity index is <0.6 in all the studied cases (**Table S3**). The absence of aggregates/agglomerates was checked by HR-SEM **(Figure S6)**. Maiorano et al. (2010) and Boldeiu et al. (2019) also confirmed by DLS and TEM analysis the single and isolated NPs and no presence of aggregates/agglomerates in these media [6,12]. Moreover, a hydrodynamic diameter increase was observed immediately (no incubation time) in presence of both media (**Table S3**), showing similar size distribution profile **(Figure S7)**. The increase in size could be attributed to proteins adsorbed onto the NP surface. This finding was reported in other studies with different types of AuNPs dispersed in these media [6,12]. The effect of incubation time at 24 h (37 ºC) was also studied. The size increases at longer incubation times leading to slightly higher values in RPMI-1640 than in DMEM-high glucose (**Table S3**). Nevertheless, Maiorano et al. (2010) described large protein corona in DMEM-high glucose [6]. Anyway, we should be cautious in the interpretation of DLS results because the presence of unbound proteins in the media can interfere with the scattering signal [33].

A specific procedure (described in section 2.4), which included purification by a centrifugation step, was used to study the hard corona [10]. This nano-biological entity was studied by incubation (1 h at 37 ˚C) of 30 nm PtNPs in DMEM-high glucose and RPMI-

1640 (**Table S3**). The Z-average size of NP was higher in RPMI than in DMEM. This size increase can be attributed to protein corona formation around these nano-sized particles. There is no evidence of aggregation because polydispersity indexes were low (<0.4) in all cases, indicating the stability of NPs dispersed in different media. HR-SEM images showed a size increase for NP in both media (98±5, and 140±12 (n=10) for DMEM and RPMI-1640, respectively), and absence of agglomerates/aggregates **(Figure S8)**. A similar study was carried out by Casals et al. (2010) with 10 nm AuNP in DMEM-low glucose (1,000 mg L^{-1} glucose and 10% FBS) and analyses by DLS before and after purification (centrifugation and precipitation) [34]. An increase in NP hydrodynamic radius was ascribed to the molecules absorbed on its surface. Also, the authors suggested that after 48 incubation the protein corona was composed of the hard and soft phases which can prevent agglomeration of the particles in the media. More recently, Piella et al. (2017) examined by the combined use of UV−vis spectroscopy, DLS, and zeta potential measurements, the formation of hard corona on the surface of AuNPs from 3.5 to 150 nm incubated in DMEM-high glucose [35]. They reported that the initial binding of the proteins was followed by a series of movements, getting a stable and irreversible interaction, and that the thickness of the protein coating was strongly dependent on the particle size.

Considering the different incubation timings used in the present work for the study of soft (0, and 24 h), and hard (1 h) protein corona, a direct comparison is not possible. A dedicated study of the time evolution would be recommended in further studies to have a closer insight to these dynamic processes. In any case, an increase in the hydrodynamic diameter of NPs occurs, giving to new hybrid nanobiostructures. It is these entities that interact with cells and trigger physiological responses, so the processes studied in this work are of major interest in toxicological field.

4. Conclusions

An analytical methodology based on the use of hybrid techniques, such as HPLC-ICP-TQ-MS, has been developed and applied for the detection and characterization of 5

and 30 nm PtNPs, as well as ionic Pt species in different cell culture media (various DMEM, and RPMI-1640 suspensions supplemented with FBS and antibiotics) commonly used in in vitro toxicological studies. Chromatographic and acquisition conditions were optimized to achieve the separation of these nano-sized particles and their corresponding ion in less than 8 min with detection limits at ppb level and adequate recoveries. The presence of cell culture media induced important transformations in PtNPs, such as oxidation and formation of new nano(bio)entities, the so-called protein corona. Regarding this last process, DLS and HR-SEM allowed to have a closer insight to distinguish hard and soft corona. Moreover, it was found that the observed transformations depend on the type of cell culture media and the incubation times selected in the experiments. These changes in the PtNPs may alter the biological process in which they are involved and hence the response in cellular models. Therefore, they should be taken into account in the interpretation of toxicological results and to do so, analytical tools like the one developed herein are of major interest.

Acknowledgments

The authors would like to thank the Spanish Ministerio de Ciencia e Innovación for financial support through the project PID2019-104381GB-I00, and the AEI/FEDER UE (ECQ2018-004010-P and EQC2019-005508-P) for the acquisition of the ICP-TQ-MS system and DLS.

Sergio Fernández-Trujillo also thanks Junta de Comunidades de Castilla-La Mancha for his pre-doctoral contract, SBPLY/16/180501/000356.

References

[1] D. Pedone, M. Moglianetti, E. De Luca, G. Bardi, P.P. Pompa, Platinum nanoparticles in nanobiomedicine, Chem. Soc. Rev. 46(16) (2017) 4951-4975.

[2] M. Jeyaraj, S. Gurunathan, M. Qasim, M. H. Kang., J. H. Kim, A comprehensive review on the synthesis, characterization, and biomedical application of platinum nanoparticles, Nanomaterials. 9(12) (2019) 1719.

[3] E. Czubacka, S. Czerczak, Are platinum nanoparticles safe to human health?, Med. Pr. 70(4) (2019) 487-495.

[4] C. F. Jones, D. W. Grainger, In vitro assessments of nanomaterial toxicity, Adv. Drug Deliv. Rev. 61(6), (2009) 438-456.

[5] S. A. Love, M. A. Maurer-Jones, J. W. Thompson, Y. S. Lin, C. L. Haynes, Assessing nanoparticle toxicity, Annu. Rev. Anal. Chem. 5 (2012) 181-205.

[6] G. Maiorano, S. Sabella., B. Sorce, V. Brunetti, M. A. Malvindi, R. Cingolani, P. P. Pompa, Effects of cell culture media on the dynamic formation of protein−nanoparticle complexes and influence on the cellular response, ACS Nano. 4(12) (2010) 7481-7491.

[7] E. Bolea, J. Jimenez-Lamana, F. Laborda, I. Abad-Alvaro, C. Blade, L. Arola, J. R. Castillo, Detection and characterization of silver nanoparticles and dissolved species of silver in culture medium and cells by AsFlFFF-UV-Vis-ICPMS: application to nanotoxicity tests, Analyst. 139(5) (2014) 914-922.

[8] S. López-Sanz, N. R. Fariñas, R. S. Vargas, R. D. C. R. Martín-Doimeadios, Á. Ríos, Methodology for monitoring gold nanoparticles and dissolved gold species in culture medium and cells used for nanotoxicity tests by liquid chromatography hyphenated to inductively coupled plasma-mass spectrometry, Talanta. 164 (2017) 451-457.

[9] S. López-Sanz, N. R. Fariñas, R. D. C. R. Martín-Doimeadios, Á. Ríos, Analytical strategy based on asymmetric flow field flow fractionation hyphenated to ICP-MS and complementary techniques to study gold nanoparticles transformations in cell culture medium, Anal. Chim. Acta, 1053 (2019a) 178-185.

[10] K. Strojan, A. Leonardi, V. B. Bregar, I. Križaj, J. Svete, M. Pavlin, M, Dispersion of nanoparticles in different media importantly determines the composition of their protein corona, PLoS one. 12(1) (2017) e0169552.

[11] J. Malejko, N. Świerżewska, A. Bajguz, B. Godlewska-Żyłkiewicz, Method development for speciation analysis of nanoparticle and ionic forms of gold in biological samples by high performance liquid chromatography hyphenated to inductively coupled plasma mass spectrometry, Spectrochim. Acta B. 142 (2018) 1-7.

[12] A. Boldeiu, M. Simion, I. Mihalache, A. Radoi, M. Banu, P. Varasteanu, P. Nadejde, E. Vasile, A. Acasandrei, R. C. Popescu, D. Savu, M. Kusko, Comparative analysis of honey and citrate stabilized gold nanoparticles: In vitro interaction with proteins and toxicity studies, J. Photochem. Photobiol. B, Biol. 197 (2019) 111519.

[13] X. Cai, X. Liu, J. Jiang, M. Gao, W. Wang, H. Zheng, S. Xu, R. Li, Molecular mechanisms, characterization methods, and utilities of nanoparticle biotransformation in nanosafety assessments, Small. 16(36) (2020) 1907663.

[14] J. M. Costa-Fernández, M. Menéndez-Miranda, D. Bouzas-Ramos, J. R. Encinar, A. Sanz-Medel, Mass spectrometry for the characterization and quantification of engineered inorganic nanoparticles, Trends Analyt Chem. 84 (2016) 139-148.

[15] S. Fernández-Trujillo, M. Jiménez-Moreno, Á. Ríos, R. D. C. R. Martín-Doimeadios, A rapid and simple approach for the characterization and quantification of gold nanoparticles in cell culture medium by single particle-ICP-MS, J. Anal. At. Spectrom. 36, (2021a) 528-534.

[16] S. Fernández-Trujillo, M. Jiménez-Moreno, Á. Ríos, R. D. C. R. Martín-Doimeadios, A simple analytical methodology for platinum nanoparticles control in complex clinical matrices via SP-ICP-MS, Talanta. 231 (2021b) 122370.

[17] F. Laborda, E. Bolea, G. Cepriá, M. T. Gómez, M. S. Jiménez, J. Pérez-Arantegui, J. R. Castillo, Detection, characterization and quantification of inorganic engineered nanomaterials: A review of techniques and methodological approaches for the analysis of complex samples, Anal. Chim. Acta. 904 (2016) 10-32.

[18] F. Laborda, A. C. Gimenez-Ingalaturre, E. Bolea, J. R. Castillo, About detectability and limits of detection in single particle inductively coupled plasma mass spectrometry, Spectrochim. Acta B. (2020) 105883.

[19] S. López-Sanz, F. J. Guzmán-Bernardo, R. D. C. R. Martín-Doimeadios, Ríos, Analytical metrology for nanomaterials: Present achievements and future challenges, Anal. Chim. Acta. 1059 (2019b) 1-15.

[20] B. Michalke, I. Vinković-Vrček, Speciation of nano and ionic form of silver with capillary electrophoresis-inductively coupled plasma mass spectrometry, J. Chromatogr. A. 1572 (2018) 162-171.

[21] Y. Yang, L. Luo, H. P. Li, Q. Wang, Z. G. Yang, Z. P. Qu, R. Ding, Analysis of metallic nanoparticles and their ionic counterparts in complex matrix by reversed-phase liquid chromatography coupled to ICP-MS, Talanta. 182 (2018) 156-163.

[22] R. Á. F. García, N. Fernández-Iglesias, C. López-Chaves, C. Sánchez-González, J. Llopis, M. Montes-Bayón, J. Bettmer, Complementary techniques (spICP-MS, TEM, and HPLC-ICP-MS) reveal the degradation of 40 nm citrate-stabilized Au nanoparticles in rat liver after intraperitoneal injection, J. Trace Elem. Med. Biol. 55 (2019) 1-5.

[23] A. Helfrich, W. Brüchert, J. Bettmer, Size characterisation of Au nanoparticles by ICP-MS coupling techniques, J. Anal. At. Spectrom. 21(4) (2006) 431-434.

[24] A. Helfrich, J. Bettmer, J, Analysis of gold nanoparticles using ICP-MS-based hyphenated and complementary ESI-MS techniques, Int. J. Mass Spectrom. 307(1-3) (2011) 92-98.

[25] C. A. Sötebier, S. M. Weidner, N. Jakubowski, U. Panne, J. Bettmer, Separation and quantification of silver nanoparticles and silver ions using reversed phase high performance liquid chromatography coupled to inductively coupled plasma mass spectrometry in combination with isotope dilution analysis, J. Chromatogr. A. 1468 (2016) 102-108.

[26] J. Soto-Alvaredo, C. López-Chaves, C. Sánchez-González, M. Montes-Bayón, J. Llopis, J. Bettmer, Speciation of gold nanoparticles and low-molecular gold species in Wistar rat tissues by HPLC coupled to ICP-MS, J. Anal. At. Spectrom. 32(1) (2017) 193-199.

[27] J. Kruszewska, D. Kulpińska, I. Grabowska-Jadach, M. Matczuk, Joint forces of direct, single particle, CE–and HPLC–inductively coupled plasma mass spectrometry techniques for the examination of gold nanoparticle accumulation, distribution and changes inside human cells, Metallomics. 12(3) (2020) 408-415.

[28] J. Soto-Alvaredo, M. Montes-Bayón, J. Bettmer, Speciation of silver nanoparticles and silver (I) by reversed-phase liquid chromatography coupled to ICPMS, Anal. Chem. 85(3) (2013) 1316-1321.

[29] X. X. Zhou, R. Liu, F. J. Liu, Rapid chromatographic separation of dissoluble Ag (I) and silver-containing nanoparticles of 1–100 nanometer in antibacterial products and environmental waters, Environ. Sci. Technol. 48(24) (2014) 14516-14524.

[30] A. Sánchez-Cachero, S. López-Sanz, N. R. Fariñas, Á. Ríos, R. D. C. R. Martín-Doimeadios, A method based on asymmetric flow field flow fractionation hyphenated to inductively coupled plasma mass spectrometry for the monitoring of platinum nanoparticles in water samples, Talanta. 222, (2021) 121513.

[31] T. Kopac, Protein corona, understanding the nanoparticle–protein interactions and future perspectives: A critical review, Int. J. Biol. Macromol. 169 (2021) 290-301.

[32] R. K. Mishra, A. Ahmad, A. Vyawahare, P. Alam, T. H. Khan, R. Khan, Biological effects of formation of protein corona onto nanoparticle, Int. J. Biol. Macromol. 175 (2021) 1-18.

[33] R. García-Álvarez, M. Vallet-Regí, M, Hard and Soft Protein Corona of Nanomaterials: Analysis and Relevance, Nanomaterials. 11(4) (2021) 888.

[34] E. Casals, T. Pfaller, A. Duschl, G. J. Oostingh, V. Puntes, Time evolution of the nanoparticle protein corona, ACS Nano. 4(7) (2010) 3623-3632.

[35] J. Piella, N. G. Bastús, V. Puntes, Size-dependent protein–nanoparticle interactions in citrate-stabilized gold nanoparticles: the emergence of the protein corona, Bioconjugate Chem. 28(1) (2017) 88-97.

Legends to figures

Figure 1. HPLC-ICP-TQ-MS chromatogram of 5 (50 µg L^{-1}) and 30 (200 µg L^{-1}) nm PtNPs mixture, and ionic Pt (15 µg L^{-1}) diluted in mobile phase (2 mM PBS, 10 mM SDS, pH = 7.3).

Figure 2. HPLC-ICP-TQ-MS chromatograms at 0 h of exposure time of (A) 5 nm PtNPs (50 µg L^{-1}), (B) 30 nm PtNPs (200 µg L^{-1}), and (C) and ionic Pt species (15 µg L^{-1}) diluted in mobile phase (2 mM PBS, 10 mM SDS, pH = 7.3, black line) and DMEM-high glucose (grey line and secondary axis of (A) and (B)).

Figure 3. HPLC-ICP-TQ-MS chromatograms at 0 h of exposure time of (A) 5 nm (50 µg L^{-1}), and (B) 30 nm (200 µg L^{-1}) PtNPs diluted in different culture media: DMEM-high glucose, DMEM F-12, DMEM 31053-028, and RPMI-1640. Standards in mobile phase are shown as vertical lines for better understanding.

Figure 4. HPLC-ICP-TQ-MS chromatograms of 5 nm PtNPs (50 µg L^{-1}) in presence of (A) DMEM-high glucose, and (B) RPMI-1640 at different incubation times: 0, 24, 48, and 96 h. Standards in mobile phase are shown as vertical lines for better understanding.

Highlights

- HPLC-ICP-TQ-MS method for the study of PtNPs and Pt ion in cell culture media.
- Oxidation processes of 5 and 30 nm PtNPs are shown in cell culture media.
- The hard and soft protein corona formation was confirmed by complementary techniques.
- Transformations of PtNPs in cell culture media should be considered in toxicology.

CRediT authorship contribution statement

Sergio Fernández-Trujillo:

Data curation, Formal analysis, Investigation, Methodology, Validation, Writing - original draft, Writing - review & editing.

Nuria Rodríguez-Fariñas:

Conceptualization, Supervision, Visualization, Formal analysis, Methodology, Writing - review & editing.

María Jiménez-Moreno:

Conceptualization, Supervision, Visualization, Methodology, Writing -review & editing.

Rosa del Carmen Rodríguez Martín-Doimeadios:

Conceptualization, Supervision, Visualization, Methodology, Writing - review & editing, Resources, Project administration, Funding acquisition.

Table 1. Optimum HPLC-ICP-TQ-MS instrumental conditions.

HPLC		
	Column	Nucleosil 7 µm particle size, C18, 1000 Å pore size, 250×4.6 mm
	Mobile phase	Phosphate Buffer (2 mM), pH = 7.3, SDS 10 mM
	Flow rate	0.5 mL min^{-1}
	Injection volume	20 µL
ICP-TQ-MS		
	RF-Power (KW)	1.5
	Plasma gas flow rate (L min^{-1})	14
	Carrier gas flow rate (L min^{-1})	0.95
	Nebulizer flow rate (L min^{-1})	0.9
	Auxiliary gas flow rate (L min^{-1})	0.8
	Spray chamber	Quartz cyclonic
	Nebulizer	MicroMist quartz nebulizer 0.4 mL min^{-1}, pumped at 40 rpm
	Isotopes monitored	^{195}Pt, ^{103}Rh
	Dwell time (ms)	100
	Mode	SQ-KED
	Gas Flow He (mL min^{-1})	4.9
	Q1 Bias (V)	-2.5
	QCell Bias (V)	-2.0
	Q3 Bias (V)	-1.0

Table 2. Analytical figures of merit without and with DMEM-high glucose.

Species	Linear range ($\mu g\ L^{-1}$)	Without		With	
		Correlation curve	LOD – LOQ ($\mu g\ L^{-1}$)	Correlation curve	LOD – LOQ ($\mu g\ L^{-1}$)
5 nm PtNP	50-500	y = 0.0079x + 0.1746; R^2=0.9999	1.3 – 4.5	y = 0.001x + 0.0092; R^2=0.9994	13.3 – 44.4
30 nm PtNP	50-500	y = 0.0037x + 0.6532; R^2=0.9995	2.4 – 7.9	y = 0.00009x + 0.01487; R^2=0.9964	14.1 – 47.1
Ionic Pt	10-25	y = 0.0081x + 0.0167; R^2=0.9996	0.3 – 0.9	y = 0.0065x + 0.0148; R^2=0.9994	2.0 – 6.5

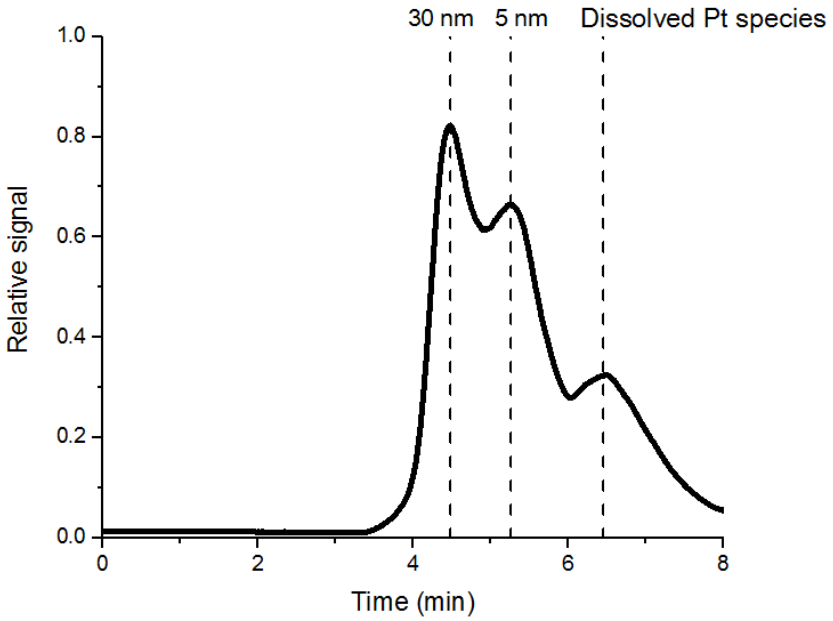

Fig. 1. HPLC-ICP-TQ-MS chromatogram of 5 (50 µg L^{-1}) and 30 (200 µg L^{-1}) nm PtNPs mixture, and ionic Pt (15 µg L^{-1}) diluted in mobile phase (2 mM PBS, 10 mM SDS, pH = 7.3).

(A)

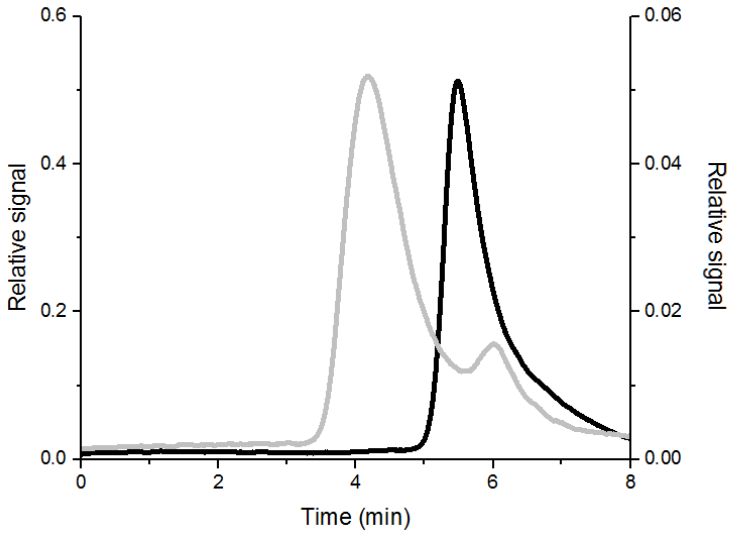
Relative signal
Relative signal
Time (min)
0.0
0.2
0.4
0.6
0.00
0.02
0.04
0.06
0
2
4
6
8

(B)

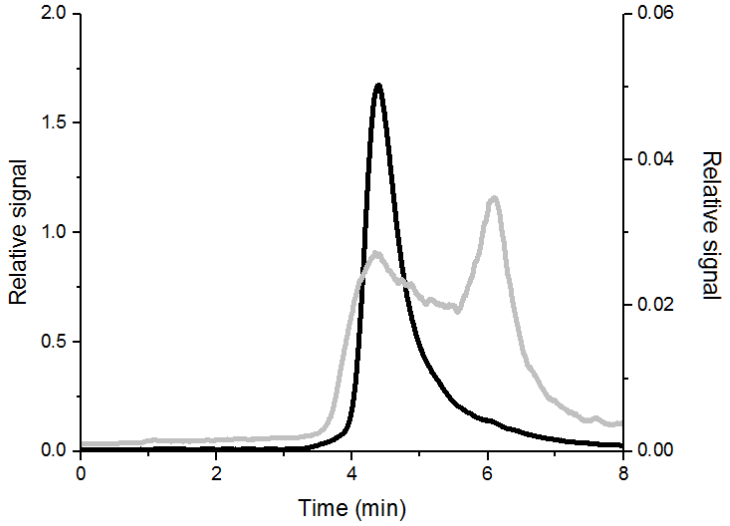
Relative signal
Relative signal
Time (min)
0.0
0.5
1.0
1.5
2.0
0.00
0.02
0.04
0.06
0
2
4
6
8

(C)

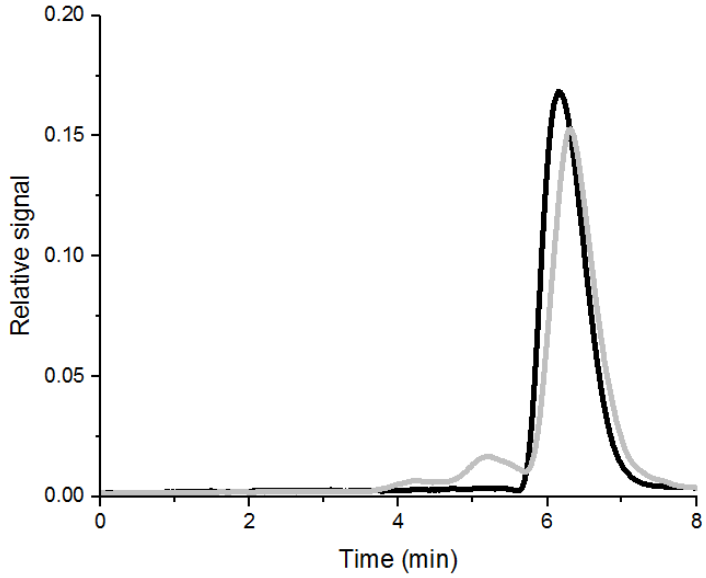

Fig. 2. HPLC-ICP-TQ-MS chromatograms at 0 h of exposure time of (A) 5 nm PtNPs (50 µg L^{-1}), (B) 30 nm PtNPs (200 µg L^{-1}), and (C) and ionic Pt species (15 µg L^{-1}) diluted in mobile phase (2 mM PBS, 10 mM SDS, pH = 7.3, black line) and DMEM-high glucose (grey line and secondary axis of (A) and (B)).

(A)

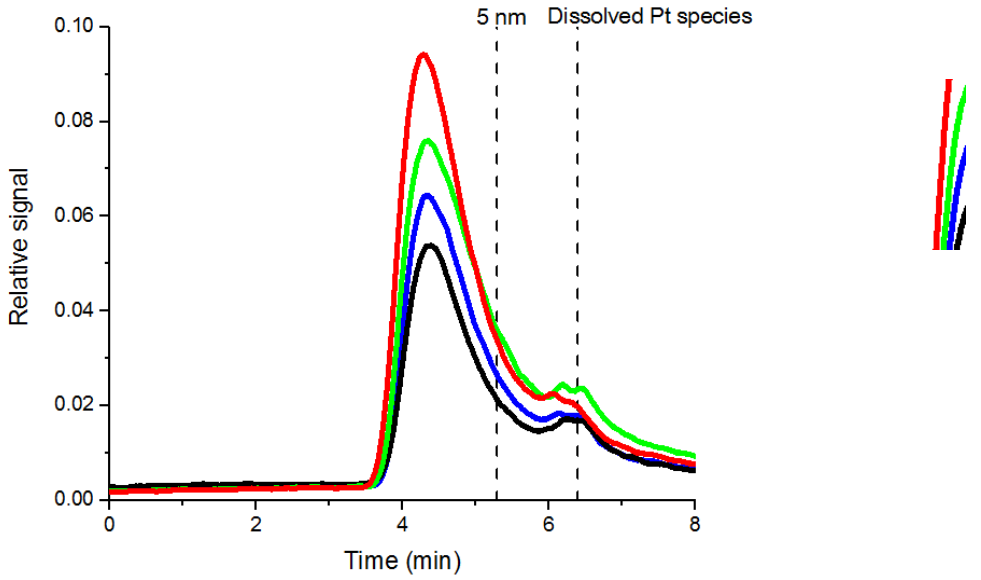

(B)

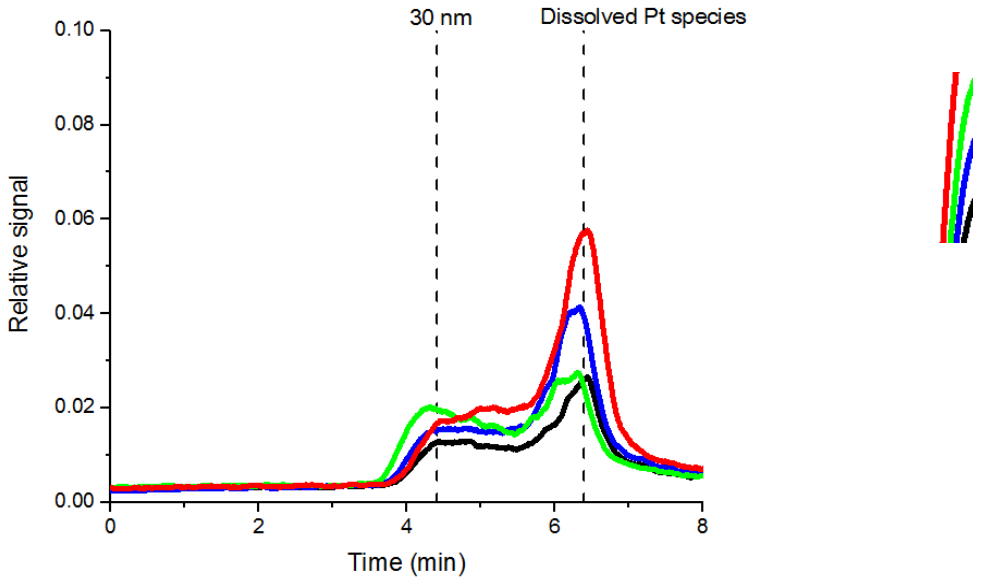

Fig. 3. HPLC-ICP-TQ-MS chromatograms at 0 h of exposure time of (A) 5 nm (50 µg L^{-1}), and (B) 30 nm (200 µg L^{-1}) PtNPs diluted in different culture media: DMEM-high glucose, DMEM F-12, DMEM 31053-028, and RPMI-1640. Standards in mobile phase are shown as vertical lines for better understanding.

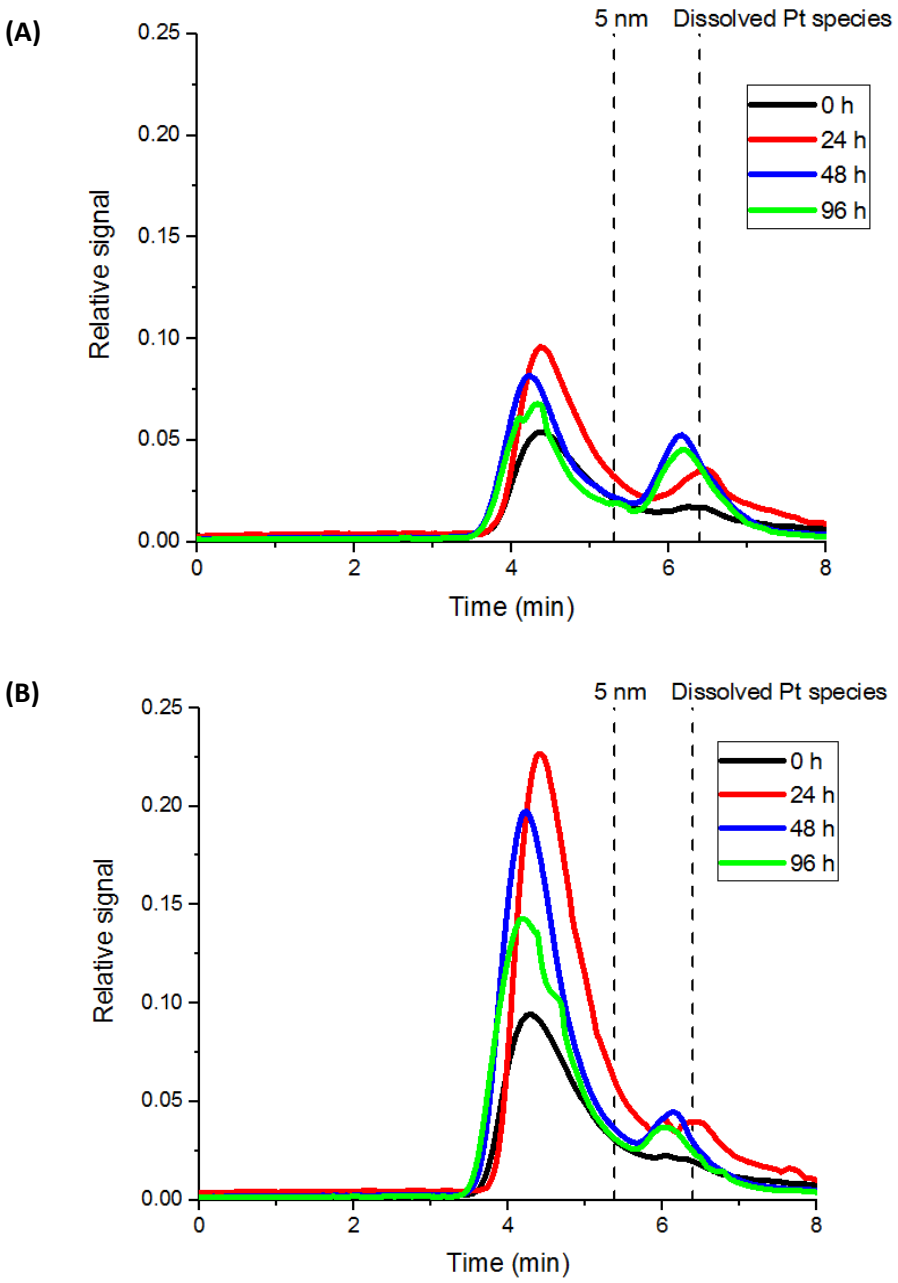

Fig. 4. HPLC-ICP-TQ-MS chromatograms of 5 nm PtNPs (50 µg L^{-1}) in presence of (A) DMEM-high glucose, and (B) RPMI-1640 at different incubation times: 0, 24, 48, and 96 h. Standards in mobile phase are shown as vertical lines for better understanding.

Table 1. Optimum HPLC-ICP-TQ-MS instrumental conditions.

HPLC		
	Column	Nucleosil 7 µm particle size, C18, 1000 Å pore size, 250×4.6 mm
	Mobile phase	Phosphate Buffer (2 mM), pH = 7.3, SDS 10 mM
	Flow rate	0.5 mL min^{-1}
	Injection volume	20 µL
ICP-TQ-MS		
	RF-Power (KW)	1.5
	Plasma gas flow rate (L min^{-1})	14
	Carrier gas flow rate (L min^{-1})	0.95
	Nebulizer flow rate (L min^{-1})	0.9
	Auxiliary gas flow rate (L min^{-1})	0.8
	Spray chamber	Quartz cyclonic
	Nebulizer	MicroMist quartz nebulizer 0.4 mL min^{-1}, pumped at 40 rpm
	Isotopes monitored	^{195}Pt, ^{103}Rh
	Dwell time (ms)	100
	Mode	SQ-KED
	Gas Flow He (mL min^{-1})	4.9
	Q1 Bias (V)	-2.5
	QCell Bias (V)	-2.0
	Q3 Bias (V)	-1.0

Table 2. Analytical figures of merit without and with DMEM-high glucose.

Species	Linear range ($\mu g\ L^{-1}$)	Without		With	
		Correlation curve	LOD – LOQ ($\mu g\ L^{-1}$)	Correlation curve	LOD – LOQ ($\mu g\ L^{-1}$)
5 nm PtNP	50-500	$y = 0.0079x + 0.1746$; $R^2=0.9999$	1.3 – 4.5	$y = 0.001x + 0.0092$; $R^2=0.9994$	13.3 – 44.4
30 nm PtNP	50-500	$y = 0.0037x + 0.6532$; $R^2=0.9995$	2.4 – 7.9	$y = 0.00009x + 0.01487$; $R^2=0.9964$	14.1 – 47.1
Ionic Pt	10-25	$y = 0.0081x + 0.0167$; $R^2=0.9996$	0.3 – 0.9	$y = 0.0065x + 0.0148$; $R^2=0.9994$	2.0 – 6.5

Figure 1

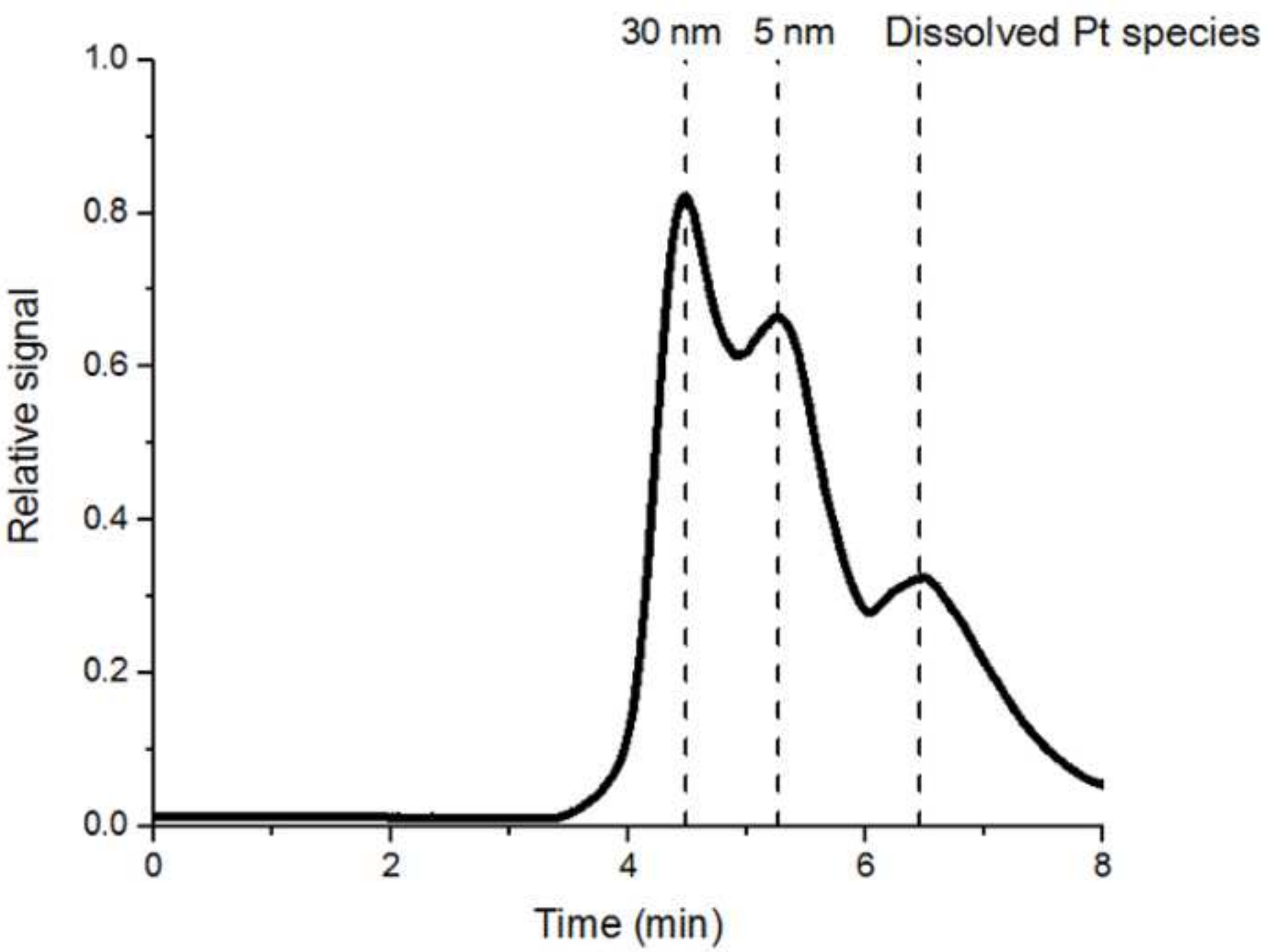

Figure 2

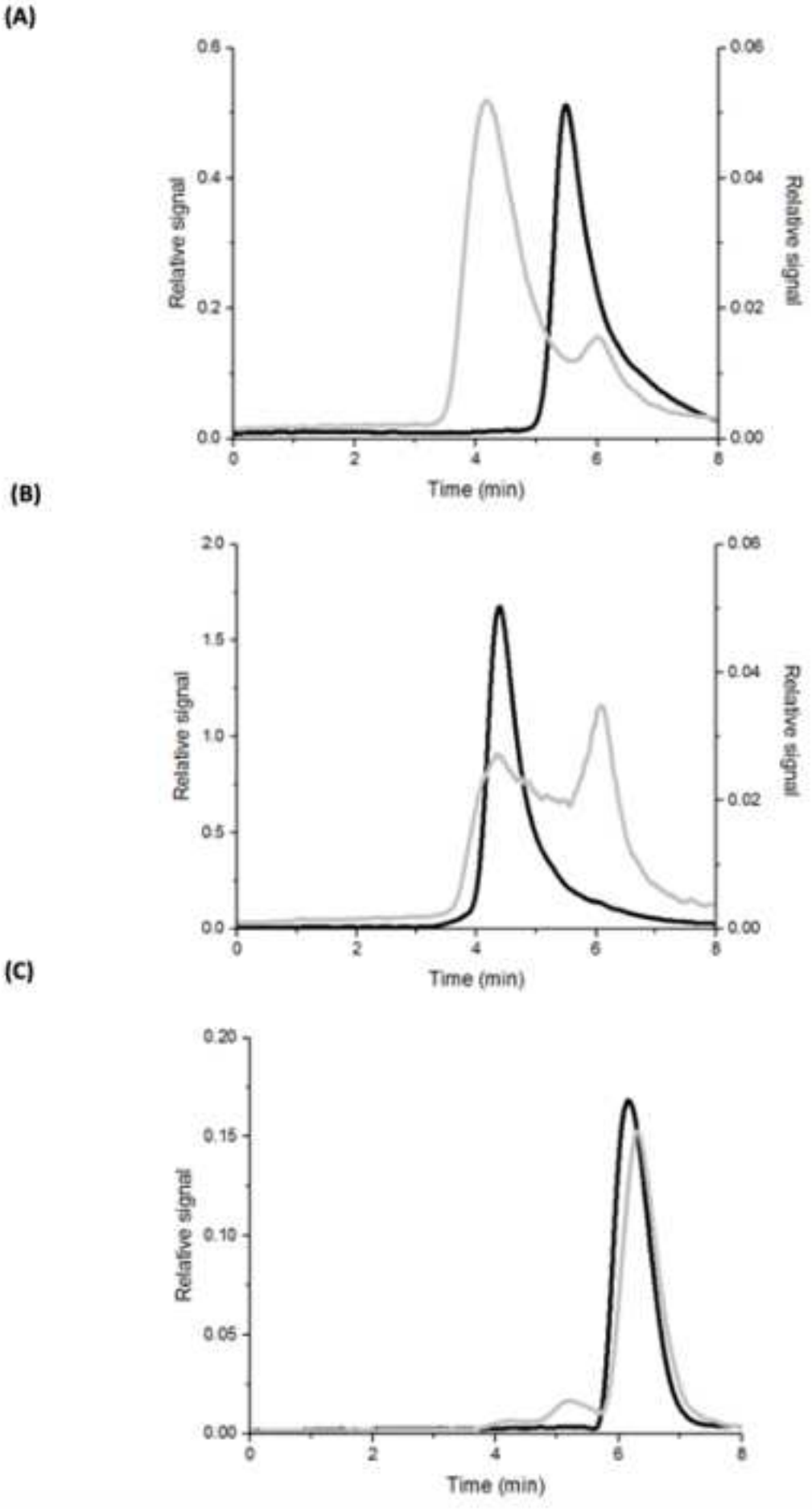

Figure 3

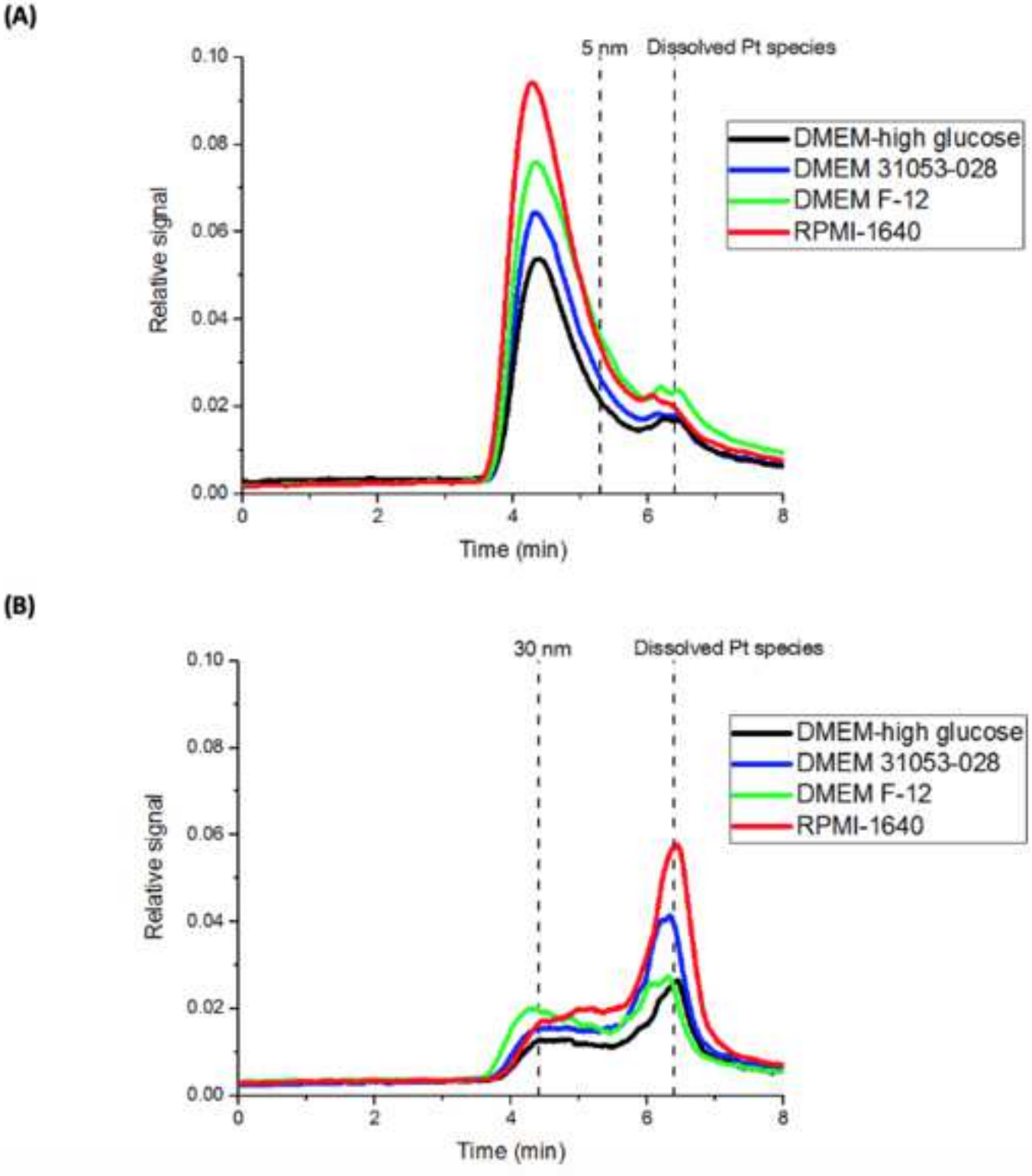

Figure 4

Click here to access/download;Figure;Figure 4.tiff